SCIENCE CHINA
Physics, Mechanics & Astronomy

• Article •
Special Issue: Physical Mechanics

June 2012 Vol.55 No.6: 1103–1110
doi: 10.1007/s11433-012-4739-0

Stochastically driven vibrations of single-layered graphene sheets

LIU RuMeng & WANG LiFeng*

State Key Laboratory of Mechanics and Control of Mechanical Structures, Nanjing University Aeronautics and Astronautics, Nanjing 210016, China

Received December 30, 2011; accepted March 31, 2012; published online April 18, 2012

Thermal vibration of single-layered graphene sheets (SLGSs) is investigated using plate model together with the law of equi-partition of energy and the molecular dynamics (MD) method based on the condensed-phase Optimized Molecular Potentials for Atomistic Simulation Studies (COMPASS) force field. The in-plane stiffness and Poisson ratio of SLGSs are calculated by stretching SLGSs. The effective thickness of SLGSs is obtained by the MD simulations for the thermal vibration of SLGSs through the natural frequency. The root-mean-squared (RMS) amplitudes for SLGSs of differing temperatures and boundary conditions are calculated by the MD, and are compared with the results calculated by the thin plate model together with the law of equi-partition of energy. At the center of SLGSs, the thin plate theory can predict the MD results reasonably well. For the difference of bonding structure of the edge atoms, the deviation between the MD results and plate theory becomes more readily apparent near the edges of SLGSs.

single-layered graphene sheets, thermal vibration, molecular dynamics simulation, RMS amplitude, thin plate theory, equi-partition of energy

PACS number(s): 05.04.-a, 43.40.+s, 46.40.-f, 61.46.-w, 62.30.+d

Citation: Liu R M, Wang L F. Stochastically driven vibrations of single-layered graphene sheets. Sci China-Phys Mech Astron, 2012, 55: 1103–1110, doi: 10.1007/s11433-012-4739-0

Graphene is a newly discovered carbon nanostructure which exhibits unique electronic properties and unusual mechanical properties [1]. The vibration characteristics of microscale and nanoscale structures have been the focus of research in the past several years. Liew et al. [2] proposed a continuum-based plate theory to investigate the vibration behavior of multilayered graphene sheets that are embedded in an elastic matrix. Behfar and Naghdabadi [3] have studied the vibration of multi-layered graphene sheets embedded in an elastic medium using molecular structural mechanics approach. Vibration analysis of multi-layered graphene sheets embedded in a polymer matrix employing nonlocal continuum mechanics has also been studied [4]. Gupta et al. [5] investigated the elastic properties and frequencies of free vibrations of SLGSs by using molecular mechanics with the MM3 potential. Investigations on free vibration of single- and double-layered graphene sheets by employing nonlocal continuum theory and molecular dynamics simulations [6] as well large amplitude vibrational properties of SLGSs using a nonlinear membrane model have been documented [7]. Chowdhury et al. [8] studied the transverse vibration of SLGSs and they reported that the natural frequencies of SLGSs decrease as the length increases.

The thermal vibration of carbon nanotubes was studied by experiment or molecular dynamics simulation to obtain their elastic property. Treacy et al. [9] estimated Young's modulus of isolated carbon nanotubes by measuring, in the transmission electron microscope, the amplitudes of their intrinsic thermal vibrations. Researchers [10] have presented a relationship between Young's modulus, the size and the standard deviation of the vibration amplitude at the tip

*Corresponding author (email: walfe@nuaa.edu.cn)

of a carbon nanotube at a given temperature. The intrinsic thermal vibrations of a single-walled carbon nanotube via molecular dynamics simulations have also been presented [11]. Dynamics problems in the thermal vibration of carbon nanotube through molecular dynamics method and the continuum theory including Euler–Bernoulli beam theory and Timoshenko beam theory have also been investigated [12]. To our knowledge, however, little work has been available for the validation of the continuum plate model in dealing with the stochastically driven vibration of SLGSs.

The primary objective of this paper is to study the validity of the plate model together with the law of equi-partition of energy in studying the thermal vibration, simulated by the molecular dynamics, of a SLGS in helium atmosphere.

1 Thin plate model

The SLGS in Figure 1(a) can be considered as a plate in Figure 1(b), which is a type of linear elastic, homogeneous and isotropic material structure.

Next, a thin plate placed in (x, y) plane with the length a, the width b, the thickness h, the mass density ρ, the Poisson ratio υ, and the Young's modulus E is considered. The governing equation for the vibration of a single-layered graphene sheet can therefore be expressed as [13]:

$$\frac{D}{\rho h}\nabla^4 w+\frac{\partial^2 w(x,y,t)}{\partial t^2}=0, \tag{1}$$

where w is the deflection in z direction, $D=Eh^3/12(1-\upsilon^2)$ is the bending stiffness.

1.1 Four edges simply-supported square plate

Suppose that all of the edges of the sheet are simply-supported, and then the deflection of the layer can be approximated by a harmonic solution of the form [13]:

$$\begin{aligned} w_{mn}^{SSSS}(x,y,t) &= A_{mn}^{SSSS}W_{mn}^{SSSS}(x,y)\mathrm{e}^{\mathrm{i}\omega t} \\ &= A_{mn}^{SSSS}\sin\frac{m\pi x}{a}\sin\frac{n\pi y}{b}\mathrm{e}^{\mathrm{i}\omega t}, \end{aligned} \tag{2}$$

where $i\equiv\sqrt{-1}$, ω is the natural frequency, A_{mn}^{SSSS} are unknown coefficients, and m and n are the half wave numbers in the direction of x and y, respectively. The substitution of eq. (2) into eq. (1) gives

$$\omega_{mn}^2-\frac{D}{\rho h}\left(\left(\frac{m\pi}{a}\right)^2+\left(\frac{n\pi}{b}\right)^2\right)^2=0. \tag{3}$$

Thus the thickness of the plate is

$$h=\sqrt{\frac{12\left(1-\upsilon^2\right)\rho_A\omega_{mn}^2}{\pi^4 K\left(\frac{m^2}{a^2}+\frac{n^2}{b^2}\right)^2}}, \tag{4}$$

where ρ_A is the surface density of the plate, and it equals ρh, $K=Eh$ is the in plane stiffness.

Now, let us consider the stochastic vibration of the thin plate from energy analysis. The total energy E_{mn} contained in the mn-th vibration mode can be found by calculating the elastic energy at the instant of maximum deflection when the cantilever is momentarily stationary, that is. $\mathrm{e}^{j\omega_{mn}t}=1$,

$$\begin{aligned} E_{mn}^{\text{kinetic}} &= \left[\frac{\rho_A}{2}\int_0^a\int_0^b\left(\frac{\partial w_{mn}^{SSSS}(x,y,t)}{\partial t}\right)^2\right]_{t=\pi/\omega_{mn}} \\ &= \frac{\rho_A}{2}\int_0^a\int_0^b\left(A_{mn}^{SSSS}\omega_{mn}\sin\frac{m\pi x}{a}\sin\frac{n\pi y}{b}\right)^2\mathrm{d}x\mathrm{d}y \\ &= \frac{\rho_A\left(A_{mn}^{SSSS}\right)^2\omega_{mn}^2 ab}{8} \\ &= \frac{\rho\left(A_{mn}^{SSSS}\right)^2 ab}{8}\left[\frac{D}{\rho}\left(\left(\frac{m\pi}{a}\right)^2+\left(\frac{n\pi}{b}\right)^2\right)^2\right]. \end{aligned} \tag{5}$$

From the law of equi-partition energy, there is an average kinetic energy of $kT/2$ per degree of freedom for all of the relevant lateral vibration modes, where k is Boltzmann constant, T is Kelvin temperature. There are both elastic and kinetic energy degrees of freedom in a vibration mode, then on average, $\langle E_{mn}\rangle=kT$ for each vibration mode. From eq. (5) we can derive:

$$\begin{aligned} \left(A_{mn}^{SSSS}\right)^2 &= 8E_{mn}^{\text{elastic}}\Big/\rho\omega_{mn}^2 ab \\ &= 8kT\Big/\left[Dab\left(\left(\frac{m\pi}{a}\right)^2+\left(\frac{n\pi}{b}\right)^2\right)^2\right]. \end{aligned} \tag{6}$$

Then the RMS amplitude of the mn-th mode at (x,y) is given as:

$$\hat{w}_{mn}^{SSSS}(x,y)=A_{mn}^{SSSS}W_{mn}^{SSSS}(x,y). \tag{7}$$

As the vibration modes are mutually independent, the vibration profile for the combined modes is also a Gaussian

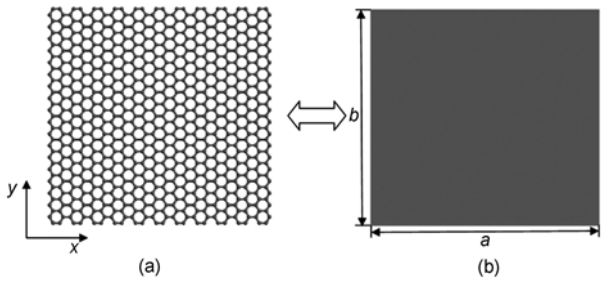

Figure 1 Models of a SLGS. (a) Molecular structure; (b) equivalent continuum structure.

distribution, with standard deviation given by the sum of the variances. The RMS amplitude of the SLGS at (x, y) is

$$\hat{w}^{SSSS}(x,y)=\sqrt{\sum_{n=1}^{\infty}\sum_{m=1}^{\infty}\left(\hat{w}_{mn}^{SSSS}\right)^2(x,y)}. \tag{8}$$

1.2 Plate with two opposite edges simply-supported and other two edges free

Suppose that two opposite edges of a plate are simply-supported and the other two opposite edges free, then the deflection of the layer can be expressed as:

$$w_{mn}^{SFSF}(x,y,t)=A_{mn}^{SFSF}W_{mn}^{SFSF}(x,y)\mathrm{e}^{\mathrm{i}\omega t}. \tag{9}$$

The classical Voigt [14,15] solution is

$$W_m^{SFSF}=\begin{bmatrix}A_m\sin\sqrt{l^2-\alpha^2}\,y+B_m\cos\sqrt{l^2-\alpha^2}\,y\\+C_m\sinh\sqrt{l^2+\alpha^2}\,y+D_m\cosh\sqrt{l^2+\alpha^2}\,y\end{bmatrix}\sin\alpha x, \tag{10}$$

where $l^4=\rho_A\omega^2/D$, $\alpha=m\pi/a$, $m=1,2,\cdots$, and where l^2 is assumed to be greater than α^2. The deflection function (10) satisfies the simply-supported boundary conditions along x=0 and x=a. Substituting eq. (10) into the free boundary conditions along the edges y=0 and y=b leads to a characteristic determinant of the fourth order for each m. Expanding the determinant and collecting terms yields a characteristic equation as follows:

$$\begin{aligned}&2\phi_1\phi_2\left[\lambda^2-m^4\pi^4(1-\upsilon)^2\right]^2(\cos\phi_1\cosh\phi_2-1)\\&+\left\{\phi_1^2\left[\lambda+m^2\pi^2(1-\upsilon)\right]^4-\phi_2^2\left[\lambda-m^2\pi^2(1-\upsilon)\right]^4\right\}\\&\times\sin\phi_1\sinh\phi_2=0.\end{aligned} \tag{11}$$

λ is the non-dimensional frequency parameter defined by

$$\lambda=\omega a^2\sqrt{\rho_A/D}. \tag{12}$$

ϕ_1 and ϕ_2 are functions of λ given by

$$\phi_1=\frac{b}{a}\sqrt{\lambda-m^2\pi^2},\quad \phi_2=\frac{b}{a}\sqrt{\lambda+m^2\pi^2}. \tag{13}$$

The coefficients in equation (10) are

$$\begin{aligned}&A_{\mathrm{m}}=\frac{\alpha_2\left(l^2+\alpha^2(\upsilon-1)\right)}{\alpha_1\left(l^2+\alpha^2(1-\upsilon)\right)}C_m,\quad B_m=\frac{\alpha_2^2-\upsilon\alpha^2}{\alpha_1^2+\upsilon\alpha^2},\\&C_m=\frac{B_m\cos\alpha_1 b\left(\alpha_1^2+\upsilon\alpha^2\right)+\cosh\alpha_2 b\left(\upsilon\alpha^2-\alpha_2^2\right)}{\sinh\alpha_2 b\left(\alpha_2^2-\upsilon\alpha^2\right)-\dfrac{\alpha_2\left(l^2+\alpha^2(\upsilon-1)\right)}{\alpha_1\left(l^2+\alpha^2(1-\upsilon)\right)}\sin\alpha_1 b\left(\alpha_1^2+\upsilon\alpha^2\right)},\\&D_m=1,\end{aligned} \tag{14}$$

where $\alpha_1=\sqrt{l^2-\alpha^2}$, $\alpha_2=\sqrt{l^2+\alpha^2}$.

The total energy E_{mn} contained in the mn-th vibration mode can be found by calculating the elastic energy at the instant of maximum deflection when the cantilever is momentarily stationary, that is, $\mathrm{e}^{j\omega_n t}=1$,

$$E_{mn}^{\mathrm{kinetic}}=\frac{\rho_A\omega_{mn}^2\left(A_{mn}^{SFSF}\right)^2}{2}\int_0^a\int_0^b\left(W_{mn}^{SFSF}\right)^2\mathrm{d}x\mathrm{d}y. \tag{15}$$

One can then calculate:

$$\begin{aligned}\left(A_{mn}^{SFSF}\right)^2&=E_{mn}^{\mathrm{kinetic}}\Big/\left[\frac{\rho_A\omega_{mn}^2}{2}\int_0^a\int_0^b\left(W_{mn}^{SFSF}\right)^2\mathrm{d}x\mathrm{d}y\right]\\&=kT\Big/\left[\frac{\rho_A\omega_{mn}^2}{2}\int_0^a\int_0^b\left(W_{mn}^{SFSF}\right)^2\mathrm{d}x\mathrm{d}y\right].\end{aligned} \tag{16}$$

The RMS amplitude of the SLGS at (x, y) can be obtained by eqs. (7) and (8) in sect 1.1.

2 MD simulation

The COMPASS force field, which has been widely employed for various gas and condensed-phase properties of many common organic and inorganic materials [16–18], is used to model the interatomic interactions. The functional form of compass force field is

$$\begin{aligned}U&=U_{nb}+U_b+U_\theta+U_\phi+U_\chi+U_{el}\\&=D_0\left[2\left(\frac{R_0}{R}\right)^9-3\left(\frac{R_0}{R}\right)^6\right]+\frac{K_b}{2}\left(R-R_0\right)^2\\&\left[1+c\left(R-R_0\right)+d\left(R-R_0\right)^2\right]\\&+\frac{K_0}{2}\left(\theta-\theta_0\right)^2\left[1+c\left(\theta-\theta_0\right)+d\left(\theta-\theta_0\right)^2\right]\\&+\frac{1}{2}\sum_j\left\{B_j\left(1+d_j\cos\left(n_j\phi-\phi_0\right)\right)\right\}+\frac{K_w}{2}w_{av}^2+C\frac{q_iq_j}{\varepsilon R},\end{aligned} \tag{17}$$

where U is total potential energy, U_{nb} is non-bonding van der Waals potential energy, U_b is stretching potential energy, U_θ is bond angle bending potential energy, U_ϕ is dihedral angle distortion potential energy, U_χ is inversion angle potential energy, U_{el} is coulomb electrostatic potential energy, R_0, R are initial and changed distance between two atoms respectively, θ_0, θ are initial and changed bond angle respectively, ϕ_0, ϕ are initial and changed dihedral angle respectively, w_{av} is inversion angle and q_i, q_j are the charge of atoms. The simulations are carried out in the (N, V, T) ensembles and the velocity-Verlet algorithm with time step 1fs is used. The Berendsen feedback thermostat [19] is employed for this system.

To determine in plane stiffness K and Poisson ratio υ of a SLGS in Figure 2, a positive displacement ΔL in the x di-

rection is applied to the carbon atoms on the right edge, then the carbon atoms on both left and right edges are fixed. The system is then relaxed. The in plane stiffness can be calculated by

$$K=\frac{1}{ab}\frac{\partial^2 U}{\partial \varepsilon^2}, \tag{18}$$

where a is the length along x direction, b is the width along y direction, U is the strain energy, the tensile strain ε is determined by $\varepsilon=\Delta L/a$. In plane stiffness K is obtained to be 357 N m based on eq. (18) by fitting U-ε curve. The Poisson ratio υ is found to be 0.3 through measuring the change of the width and the length of the SLGS.

In order to simulate the thermal vibration of SLGS in helium atmosphere, a periodic lattice filled with atoms of helium is built, and the distance between two atoms of helium is given as 0.8 nm. A piece of SLGS with length a=4.97 nm and width b=3.2 nm is embedded into this periodic lattice, and the boundary carbon atoms on all-around are fixed. The free thermal vibration of the system is simulated by the MD after it is fully relaxed (see in Figure 3).

The histories of one random inner atom are recorded for a certain duration as shown in Figure 4(a), and then the natural frequencies are computed by using the fast Fourier transform (FFT) method. As shown in Figure 4(b), every peak represents one natural frequency of the SLGS.

Figure 5 shows the first natural frequencies of the SLGS in different temperatures. From Figure 5, we can see that the nature frequencies of the SLGSs almost keep constant when the temperature changes from 50 K to 500 K. The effects of temperature can be considered as a random excitation to the

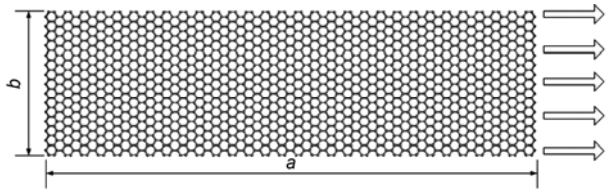

Figure 2 SLGS for tensile test.

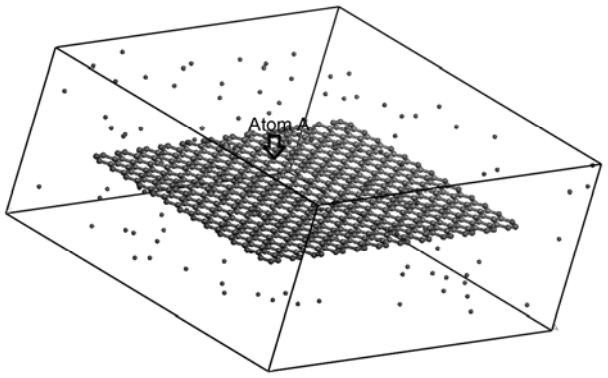

Figure 3 SLGSs (a=4.97 nm, b=3.2 nm) with four edges simply-supported in a helium atmosphere in the MD simulation.

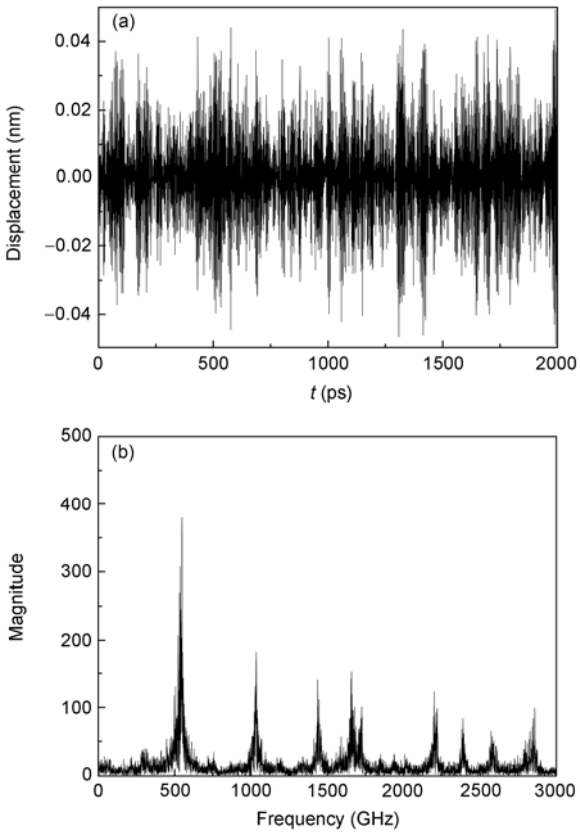

Figure 4 Displacement of atom A and FFT results. (a) Displacement in the z direction of atom A in Figure 3 by the MD simulation; (b) amplitude-frequency curve of atom A.

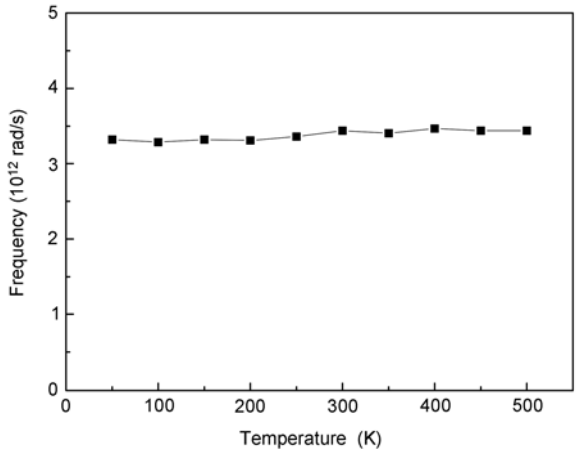

Figure 5 First natural frequencies of SLGSs (a=4.97 nm, b=3.2 nm) with four edges simply-supported at different temperatures.

vibration of SLGSs.

Altering the initial distance between two atoms of helium, we can get the natural frequencies of SLGS in different gas density atmosphere. From Figure 6, we can see that the natural frequencies of the SLGSs almost remain constant when the gas density changes.

The first natural frequency of the SLGSs can be found

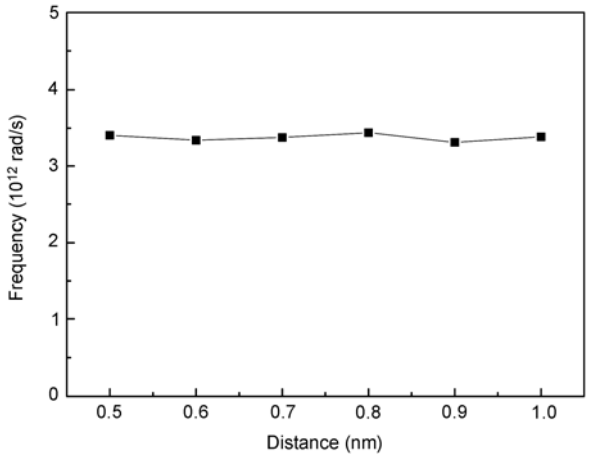

Figure 6 First natural frequencies of SLGSs (a=4.97 nm, b=3.2 nm) with four edges simply-supported in different gas density atmosphere.

from Figure 5 as ω=3.45×10^{12} rad/s. Then we can obtain the equivalent thickness of SLGSs h=0.38 nm using eq. (4). The equivalent continuum model of SLGSs is now established.

3 Comparison between analytical and MD results

The displacement in the z direction w_i, (i=1, 2, …, t) of an atom at coordinate (x, y) in the SLGSs are recorded for a certain duration t. Then RMS amplitude of the SLGSs can be expressed as:

$$\hat{w} = \sqrt{\frac{\sum_{i=1}^{t} w_i^2}{t}}. \tag{19}$$

The results calculated by the continuum model and MD method under different boundary conditions are investigated.

3.1 SLGSs with four edges simply-supported

For the SLGSs with four edges simply-supported, we calculate the RMS amplitudes of the atom in the center of SLGS in different density gas atmospheres. Figure 7 shows the results calculated by MD and plate model. The discrete square points in Figure 7 are the RMS amplitudes of the atoms in the center of SLGSs in helium atmosphere. The solid line is the RMS amplitude in the center of a SLGS obtained by plate theory. The dash-dot line is the RMS amplitude of the atom in the center of an isolated SLGS which is in vacuum. From this figure we can see that the RMS amplitudes obtained by MD of a SLGS in helium atmosphere and plate theory are consistent with each. The RMS amplitude, simulated by MD, of the atom in isolated SLGS is significantly greater than that calculated by the plate model. These results suggest that inert gas can provides better hot bath conditions than the isolated graphene.

Figure 8 shows the RMS amplitudes of the atom in the center of the SLGS by MD and thin plate model in different temperatures. The initial distance between two atoms of helium in these MD simulations is 0.8 nm. From this we can see that the thin plate theory together with the law of equipartition energy can give us good predictive results to the MD.

Figure 9 shows the RMS amplitudes of the SLGSs by the continuum model (a) and MD method (b). The shape of Figures 9(a) and 9(b) is similar. The RMS amplitudes of a number of atoms in x and y boxes in differing temperatures are shown in Figure 10. It can be seen that at the center of the box, that is in the center of the SLGS, the results calculated by the continuum models and MD simulation are consistent. However, at the edge of SLGS, the difference between the plate theory and MD results becomes obvious.

Moreover, the RMS amplitudes of SLGSs in different sizes at temperature of 300 K are obtained as shown in Figure 11. The differences between the thin plate theory and

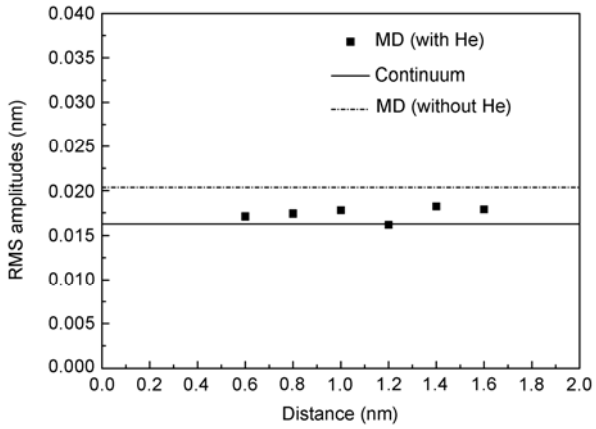

Figure 7 RMS amplitudes of SLGSs (a=4.97 nm, b=3.2 nm) with four edges simply-supported at different gas density calculated by the MD and plate model.

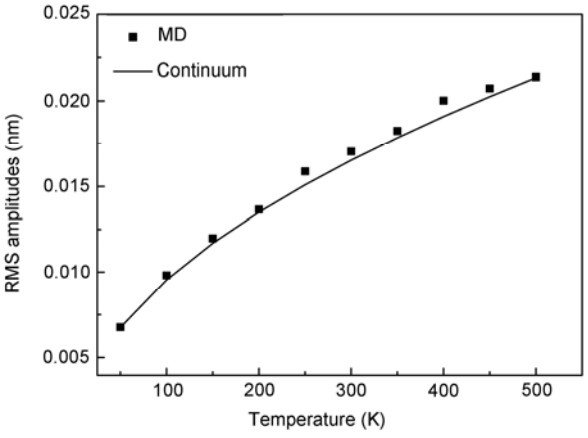

Figure 8 RMS amplitudes of SLGSs (a=4.97 nm, b=3.2 nm) with four edges simply-supported at different temperatures calculated by the MD and plate model.

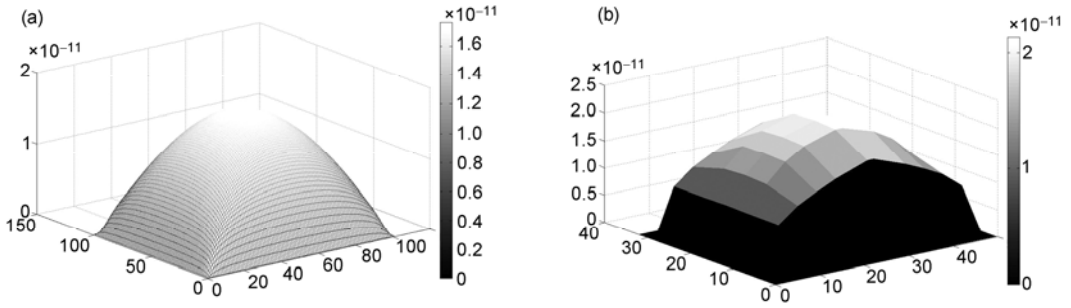

Figure 9 RMS amplitudes of SLGSs (a=4.97 nm, b=3.2 nm) with four edges simply-supported calculated by the plate model and MD method at temperature of 300 K. (a) RMS amplitudes of SLGSs calculated by the plate model; (b) RMS amplitudes of SLGSs simulated by the MD.

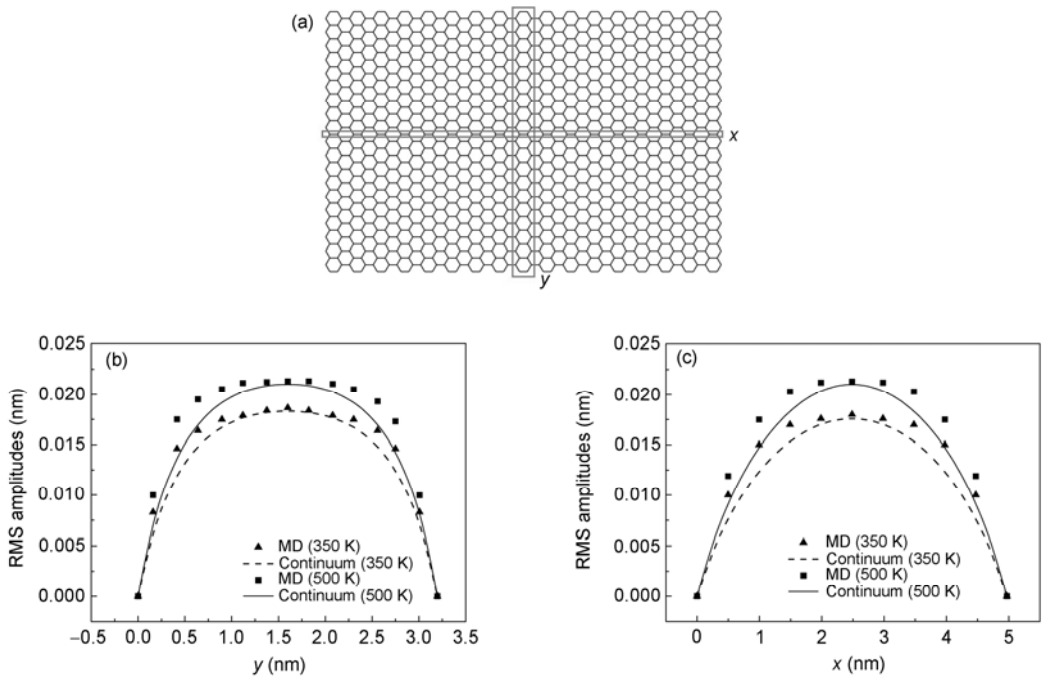

Figure 10 RMS amplitudes of SLGSs (a=4.97 nm, b=3.2 nm) with four edges simply-supported in different position calculated by the MD and plate model. (a) Position of x, y boxes on SLGS; (b) RMS amplitudes of atoms in y box calculated by the MD and plate model; (c) RMS amplitudes of atoms in x box calculated by the MD and plate model.

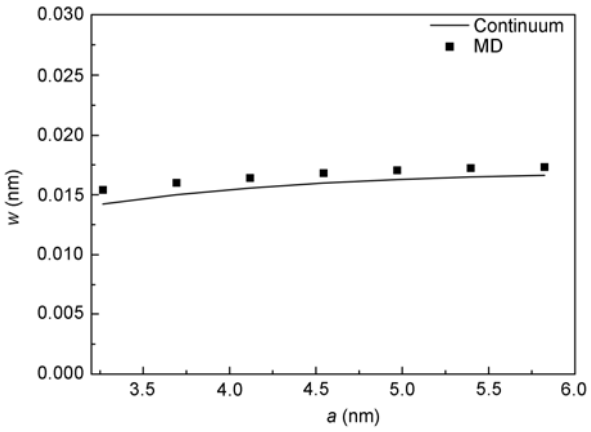

Figure 11 RMS amplitudes of SLGSs with four edges simply-supported in different sizes calculated by the MD and plate model at temperature of 300 K.

MD results gradually become obvious, when the size of graphene sheet is very small. This result may be explained by the size-effects of mechanical property SLGSs.

3.2 SLGSs with two opposite edges simply-supported and other two edges free

Figure 12 shows the RMS amplitudes of the SLGSs with the boundaries at x=0 and x=a simply-supported, and y=0 and y=b free by the continuum model (a) and MD method (b). The shape of Figures 12(a) and 12(b) is similar. However, the curves of the free edges obtain by the MD simulation are not considered smooth. Figure 13 shows the RMS amplitudes along y-axis of a SLGS with length a=4.4 nm and width b=4.3 nm. The RMS amplitude in the center of SLGS given by plate model is close the results by MD simulations.

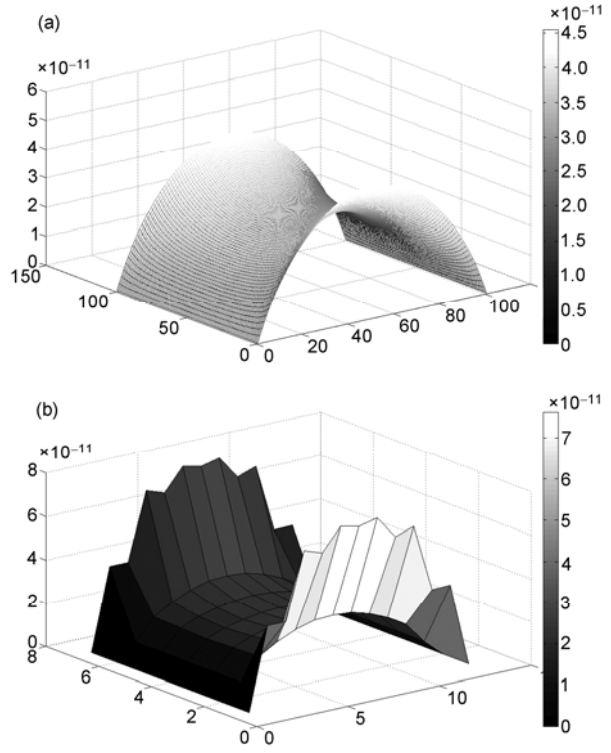

Figure 12 RMS amplitudes of SLGSs (a=4.4 nm, b=4.3 nm) with two opposite edges simply-supported and other two edges free calculated by the plate model and MD method at temperature of 300 K. (a) RMS amplitudes of SLGSs calculated by the plate model; (b) RMS amplitudes of SLGSs calculated by the MD method.

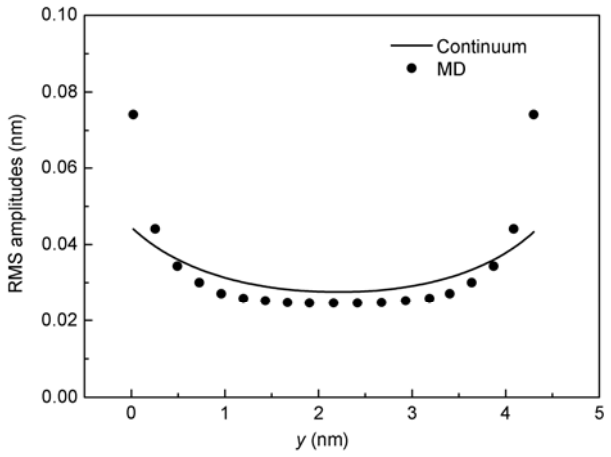

Figure 13 RMS amplitudes along y-axis of SLGSs (a=4.4 nm, b=4.3 nm) with two opposite edges simply-supported and other two edges free calculated by the MD and plate model.

Different from those inner carbon atoms which have three nearest atoms, only two atoms are nearest the atoms in the boundary. Thus the RMS amplitudes of the free edge obtained by the MD simulations are significantly greater than that obtained by the plate model.

4 Conclusions

The thermal vibrations of SLGSs under helium atmosphere are investigated using both the MD method based on the COMPASS force field potential and the thin plate model in conjunction with the law of equi-partition energy. The equivalent continuum model of SLGS is established through the determinations of the in-plane stiffness, Poisson's ratio and the effective thickness of SLGSs by the MD simulations. In the center of SLGS, the plate model together with the law of equi-partition energy can give us a reasonable prediction to the RMS amplitudes for the thermal vibrations, simulated by molecular dynamics. However, at the edge of SLGS, the difference between the plate theory and the MD results becomes more readily apparent. The RMS amplitudes obtained by the MD is significantly greater than that obtained by the plate model in the location near the free edge. These results show clear evidence of edge effects of SLGSs.

This work was supported by the National Natural Science Foundation of China (Grant Nos. 11072108), the Foundation for the Author of National Excellent Doctoral Dissertation of China (Grant No. 201028), Program for New Century Excellent Talents in University (Grant No. NCET-11-0832) and the Foundation of Nanjing University Aeronautics and Astronautics.

1 Novoselov K S, Geim A K, Morozov S V, et al. Electric field effect in atomically thin carbon films. Science, 2004, 306: 666–669
2 Liew K M, He X Q, Kitipornchai S. Predicting nanovibration of multi-layered graphene sheets embedded in an elastic matrix. Acta Mater, 2006, 45: 4229–4236
3 Behfar K, Naghdabadi R. Nanoscale vibrational analysis of a multi-layered graphene sheet embedded in an elastic medium. Composite Sci Tech, 2005, 65: 1159–1164
4 Pradhan S C, Phadikar J K. Small scale effect on vibration of embedded multilayered graphene sheets based on nonlocal continuum models. Phys Lett A, 2009, 373: 1062–1069
5 Gupta S S, Batra R C. Elastic properties and frequencies of free vibrations of single-layer graphene sheets. J Comput Theor Nanosci, 2010, 7: 1–14
6 Arash B, Wang Q. Vibration of single- and double-layered graphene sheets. J Nanotech Eng Med, 2011, 2: 011012
7 Mianroodi J R, Niaki S A, Naghdabadi R, et al. Nonlinear membrane model for large amplitude vibration of single layer graphene sheets. Nanotechnology, 2011, 22: 305703
8 Chowdhury R, Adhikari S, Scarpa F, et al. Transverse vibration of single-layer graphene sheets. J Phys D-Appl Phys, 2011, 44: 205401
9 Treacy M M J, Ebbesen T W, Gibson J M. Exceptionally high Young's modulus observed for individual carbon nanotubes. Nature, 1996, 381: 678–680
10 Krishnan A, Dujardin E, Ebbesen T W, et al. Young's modulus of single-walled nanotubes. Phys Rev B, 1998, 58: 14013–14019
11 Hsieh J Y, Lu J M, Huang M Y et al. Theoretical variations in the Young's modulus of single-walled carbon nanotubes with tube radius and temperature: A molecular dynamics study. Nanotechnology, 2006, 17: 3920–3924
12 Wang L F, Hu H Y, Guo W L. Thermal vibration of carbon nanotubes predicted by beam models and molecular dynamics. Proc R Soc A, 2010, 466: 2325–2340

13 Leissa A W. Vibration of Plates. NASA, 1969
14 Leissa A W. The free vibration of rectangular plates. J Sound Vib, 1973, 31(3): 257–293
15 Voigt W. Bemerkungen zu dem problem der transversalen schwingungen rechteckiger platen. Nachr Ges Wiss, 1893, 6: 225–230
16 Grujicic M, Cao G, Roy W N. Atomistic modeling of solubilization of carbon nanotubes by non-covalent functionalization with poly (p-phenylenevinylene-co-2, 5-dioctoxy-mphenylenevinylene). Appl Surf Sci, 2004, 227(1-4): 349–363
17 Sun H. COMPASS: An ab initio force-field optimized for condensed-phase applications-overview with details on alkane and benzene compounds. J Phys Chem B, 1998, 102(38): 7338–7364
18 Sun H, Ren P, Fried J R. The COMPASS force field: parameterization and validation for phosphazenes. Comput Theor Polymer Sci, 1998, 8(1-2): 229–246
19 Berendsen H J C, Postma J P M, Gunsteren W F, et al. Molecular dynamics with coupling to an external bath. J Chem Phys, 1984, 81: 3684–3690